ENGINEERING Computations

Volume 7, Number 3, September 1990
ISSN 0264–4401

Pineridge Press Limited,
54 Newton Road, Mumbles,
Swansea, SA3 4BQ U.K.

Numerical prediction of an oil-fired water tube boiler

Maria da Graça Carvalho and Pedro Jorge Coelho
Instituto Superior Técnico, Department of Mechanical Engineering, 1096 Lisbon Codex, Portugal
(*Received August 1989; revised January 1990*)

ABSTRACT

A fully three-dimensional model has been applied to an oil-fired water tube boiler in order to predict the flow, temperature, mixture fraction, species concentrations and the heat flux distributions to the furnace walls. The partial differential equations governing conservation of mass, momentum and energy as well as those describing the combustion phenomena are discretized by a finite volume method and solved numerically. Radiative heat transfer is handled by the discrete transfer method. Predicted results are presented and compared with experimental data for the heat fluxes. The results have suggested that 3-D models of the present kind can be used with some confidence for design calculations.

NOMENCLATURE

A	soot model constant
C_f	soot formation rate coefficient
$C_{p,j}$	constant pressure specific heat of species j
C_μ	constant in the turbulence model
E	activation energy
h	specific enthalpy
H	lower calorific value of the fuel
k	kinetic energy of turbulence
m_j	time-averaged mass fraction of a species j
m_s	soot mass fraction
n	soot model constant
P_{fu}	fuel partial pressure
R_0	universal gas constant
s_{fu}	stoichiometric oxidant-to-fuel ratio
s_s	stoichiometric oxidant-to-soot ratio
S_d	soot consumption rate
S_f	soot formation rate
S_ϕ	source term
T	temperature
U_j	time-averaged velocity component in j direction
x_j	coordinate in j direction
Γ_ϕ	effective diffusion coefficient
ε	dissipation rate of turbulent kinetic energy
μ_t	turbulent viscosity
ρ	time-averaged density
ϕ	generic property
ϕ	equivalence ratio (in (4))

Subscripts

fu	fuel
ox	oxidant
s	soot

INTRODUCTION

For many years the design of boiler furnaces was based on empirical methods. However, to face the rapid developments in utility boiler unit size, the requirements of high performance dictated by the energy crises and the progressively more restrictive pollution regulations, research programs were initiated. Advances in computer power allied to advances in the understanding of fluid mechanics mechanisms have given birth to the science of computational fluid dynamics.

Knowledge of the flow pattern in a boiler is important to optimize the furnace shape and to provide sufficient residence time for complete combustion of the fuel. Measurements of the flow field in laboratory-scale models of boilers were carried out by Kalmbach *et al.*[1], Shida *et al.*[2,3] and Boyd *et al.*[4] and compared with the results of mathematical models. Shida *et al.*[2,3], Boyd *et al.*[5] and Benesch *et al.*[6] made predictions of the flowfield for industrial boiler furnaces but only Boyd *et al.* present comparisons with experimental data for isothermal flow.

Heat flow and temperature distributions are useful to evaluate furnace heat transfer efficiency and to identify slagging and dryout problems. Predictions of these distributions based on flow patterns assumed or taken from experimental data were presented by Hirose *et al.*[7], Anson[8], Lowe *et al.*[9], Bueters *et al.*[10], Richter *et al.*[11], Xu-Chang[12], Sakai *et al.*[13] and Scruton *et al.*[14]. Comparisons with data generally reveal satisfactory agreement.

The aforementioned works, despite remaining useful for many purposes, calculate the flow or the heat flux distributions separately. A more powerful technique is the coupling of the fluid flow, combustion and heat and mass transfer processes

0264–4401/90/030227–08$2.00

by solving the simultaneous 3-D partial differential equations governing these phenomena. The simultaneous presence of two or more phases can also be handled by these techniques. Hence, the possibility is opening up to obtain a much more precise and detailed picture than hitherto of the phenomena occurring in combustion chambers. This can improve design of conventional equipment and more important still might stimulate new ideas of radically new designs of equipment. Robinson[15] presented the first numerical study based on an integrated treatment of flow, combustion and heat transfer for a large tangentially-fired furnace of the type used in power-station boilers. Since then, more studies of boilers by means of full 3-D mathematical models have appeared in the literature. Abbas *et al.*[16] compared predictions for the flow aerodynamics with isothermal data collected by CEGB in a scale model. Further predictions for gas temperature and wall heat transfer were presented for the same geometry when fired with a gaseous fuel. Gorner *et al.*[17] predicted the flow field, the temperature and CO_2 distributions and heat fluxes to the walls in a coal fired furnace. A simplified mechanism of pulverized coal combustion was used in the mathematical model. Velocity data obtained from an isothermal Perspex model were used for comparison. The combustion model was tested for a single enclosed flame where measurements were available. However, only a few experimental heat fluxes in the boiler were available for assessment of the full code. Boyd *et al.*[18] applied the 3-D model to a power station coal-fired boiler. Predicted temperatures, oxygen concentrations, heat fluxes and carbon burnout were in generally good agreement with the available data. Fiveland *et al.*[19] also applied the model to the prediction of a pulverized-coal combustion boiler. Predictions of the flow field, temperature distributions, oxygen concentration and heat fluxes on the walls were presented and a sensitivity analysis of the model was investigated for several parameters. However, no comparisons were made to assess the model.

The present study is intended to contribute to the assessment of full 3-D mathematical models by comparisons of predicted results with available data and to stress the usefulness of such models to enhance our understanding of the phenomena occurring in large industrial boilers.

In this study a full 3-D mathematical model was applied to a boiler converted from coal to oil firing. The model is applied only to the combustion chamber. Some authors (Shida *et al.*[2,3] and, recently, De Michele *et al.*[20]) have extended their analysis to the convective section but they used a simplified model for the combustion chamber. Predictions of the flow field, temperature, mixture fraction, species concentrations and heat fluxes are presented and discussed. Calculated heat fluxes to the walls are compared with experimental data obtained by Anson *et al.*[8].

MATHEMATICAL MODEL

The governing time-averaged transport equations for a turbulent three-dimensional flow in cartesian coordinates take the form:

$$\frac{\partial}{\partial x_j}(\rho U_j \phi) = \frac{\partial}{\partial x_j}\left(\Gamma_\phi \frac{\partial \phi}{\partial x_j}\right) + S_\phi \tag{1}$$

where ϕ is the dependent variable, Γ_ϕ is the effective diffusion coefficient, S_ϕ is a source term and index j denotes summation over the three coordinates. Equation (1) represents mass conservation when $\phi = 1$, momentum conservation when ϕ is one of the velocity components, energy conservation when ϕ is the stagnation enthalpy and a mass fraction conservation when ϕ is a mass fraction of a chemical species.

The standard k–ε turbulence model[21] is used to close the time-averaged equations of the mean flow. The turbulent viscosity is related to k and ε by dimensional arguments:

$$\mu_t = C_\mu \frac{\rho k^2}{\varepsilon} \tag{2}$$

where C_μ is a constant of the model and k and ε are calculated from their differential transport equations.

The combustion model assumes instantaneous evaporation of the fuel. Reaction rates associated with the fuel oxidation are assumed to have very short time scales compared with those describing the transport processes and so chemical equilibrium prevails. Assuming also that all species and heat diffuse at the same time, instantaneous gas composition can be determined as a function of a strictly conserved scalar variable. The mixture fraction was the scalar variable chosen for this process.

In a turbulent flow, the mixture fraction fluctuates and due to the non-linearity of the relationships, knowledge of its mean value is insufficient to allow the determination of the mean values of such quantities as density or temperature. The fluctuating nature of the turbulent reaction is accommodated through a modelled equation for the variance of the mixture fraction. We adopt a statistical approach to describe the temporal nature of the mixture fraction fluctuations. In the present work we have assumed the 'clipped' normal probability density function[22] which is completely defined by the knowledge of the mean value of the mixture fraction and its variance.

The specific mixture enthalpy may be defined by:

$$h=\int_0^T \sum m_j C_{pj}(T)\,\mathrm{d}T + m_{\mathrm{fu}} H \qquad (3)$$

where C_{pj} is the constant-pressure specific heat of a species j.

The radiative heat transfer is calculated using the 'discrete transfer' method of Lockwood and Shah[23] which is a general and numerically exact solution technique. The method is based on the direct solution of the radiation intensity transport equation. A recurrence form of this transport equation is solved in discretized solid angles within which the intensity is assumed to be uniform over the finite-difference cells of the flow calculations. The energy gain or loss within each cell can then be calculated and appended to the energy conservation equation.

The distinctive feature of oil-fired flames is their significant soot content. Soot is of concern because its presence greatly augments the radiation heat transfer and because it is a pollutant. To predict the spatial distribution of soot a transport equation of its mass concentration was solved. To characterize soot production, a global expression similar to that used by Khan and Greeves[24] was chosen:

$$S_f = C_f P_{\mathrm{fu}} \phi^n \exp(-E/R_0 T) \qquad (4)$$

where C_f although ideally being a constant depending on an easily definable fuel property such as the C/H ratio was taken as a constant[25]. A straightforward method of estimating the rate of soot burning proposed by Magnussen and Hjertager[26] was used in the present work. The soot consumption rate is given by:

$$S_d = \min\left\{ A m_s \frac{\varepsilon}{k}, \frac{m_{\mathrm{ox}}}{m_s s_s + m_{\mathrm{fu}} s_{\mathrm{fu}}} m_s \frac{\varepsilon}{k} \right\} \qquad (5)$$

where min means the minimum of the two expressions in brackets and A is a model constant. The source term in (1) is the difference $S_f - S_d$.

The gas/soot absorption coefficient is calculated using the 'mixed grey and clear' gas formulation of Hottel and Sarofim[27]. The constants and weighting coefficients determined by Truelove[28], who assumed a mixture of two grey gases plus a clear gas are employed.

NUMERICAL SOLUTION PROCEDURE

The Eulerian partial differential equations governing the transport of mass, momentum, energy and turbulent mixing are cast into finite-difference form. The control volume method used to solve the equations entails subdividing the furnace into a number of finite volumes or 'cells'. The convection terms were discretized by the hybrid central/upwind method[29]. The velocities and pressures are calculated by a variant of the SIMPLE algorithm[30]. The solution of the individual equations sets was obtained by a form of Gauss–Seidel line-by-line iteration.

THE MODELLED BOILER

The boiler examined in the present study is an oil-fired water tube boiler (*Figure 1a*) which has been converted from coal to oil firing. The overall dimensions are $24.5 \times 6 \times 9$ m^3. It has four pairs of burners arranged vertically on each side wall (16 burners in all).

The combustion air is introduced in the combustion chamber through circular openings surrounding each burner. Most of the energy released by the combustion of air and fuel is radiated to the walls covered by the water tubes. The combustion products leave the combustion chamber through an opening at the top of the back wall towards the superheaters, reheaters and economizers located in the convection section (see *Figure 1b*).

The simplified geometry of the combustion chamber is presented in *Figure 2*. It is assumed that the vertical walls where the tubes are located are at uniform temperature. This assumption is supported by the experiments of Anson *et al.*[8] who have noticed only a small variation in tube surface temperature. The small curvature of the walls due to the presence of the tubes and the detailed geometry of the burners are not accounted for and the ash hopper is modelled in a stepwise fashion. These are common approaches which are not expected to influence the general features of the predictions.

The operating conditions for this boiler were reported by Anson *et al.*[8] who measured flame emissivities, temperatures and heat fluxes to the

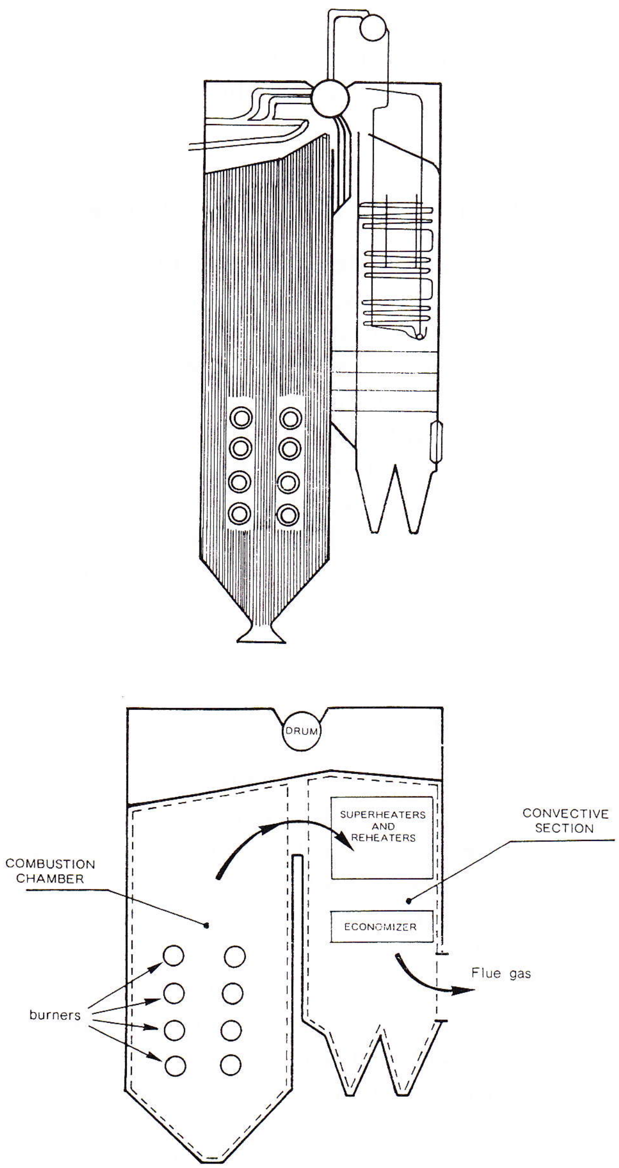

Figure 1 Sketch of the oil-fired water-tube boiler

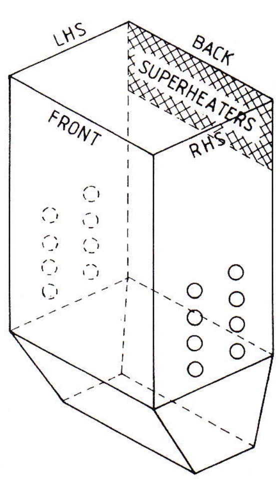

Figure 2 Simplified geometry of the combustion chamber

walls. When measurements were made only two burners of the first stage, one in each side wall, were in operation.

The computations were carried out on a $15 \times 24 \times 60$ node mesh for the flow and a $7 \times 11 \times 23$ node mesh for the radiation. The hopper region was treated in a stepwise fashion. The radiation calculation was only performed every 10 iterations. Convergence was achieved when the normalized residuals were less than 3×10^{-3} which required 420 iterations.

RESULTS AND DISCUSSION

Predicted velocity vectors in a horizontal plane passing through the third level of burners are presented in *Figure 3a*. The jets penetrate up to the middle of the furnace where frontal jets collide and are deflected partly to the front and back walls originating large recirculating regions and partly to the centre of the furnace. Since two of the burners in the first level were not in operation, one nearer the front wall and the other one nearer the back wall, the velocity field is not symmetric.

Velocity vectors predicted in a plane parallel to the front wall and passing through the burners close to this wall are shown in *Figure 3b*. Since the lower burner of the right-hand side (RHS) wall was not in operation the flow is asymmetric. The jets from the burners of the left-hand side (LHS) wall penetrate deeper before being deflected upwards towards the furnace exit to the superheaters. A large recirculating region can be identified above the upper burner plane close to the RHS wall. The hopper region is characterized by very low velocities. This can be verified in a vertical plane midway between the side walls (see *Figure 3c*). In this plane velocities increase markedly above burners towards the superheaters. No experimental data are available for the velocity field.

Figure 4 shows gas temperature distribution in the same planes where velocities are presented. The location of the burners is easily identified in *Figure 4a*. Steep gradients can be seen close to the burners and are due to oxidation and combustion of the fuel. The main features of the distribution temperature are closely related to the velocity field presented in *Figure 3a*. Both of the Figures show the penetration of the jets towards the centre of furnace where the jets collide and are deflected. Temperature distribution in the vertical planes of *Figures 4b* and *4c* show that the highest temperatures occur at the burner levels as expected

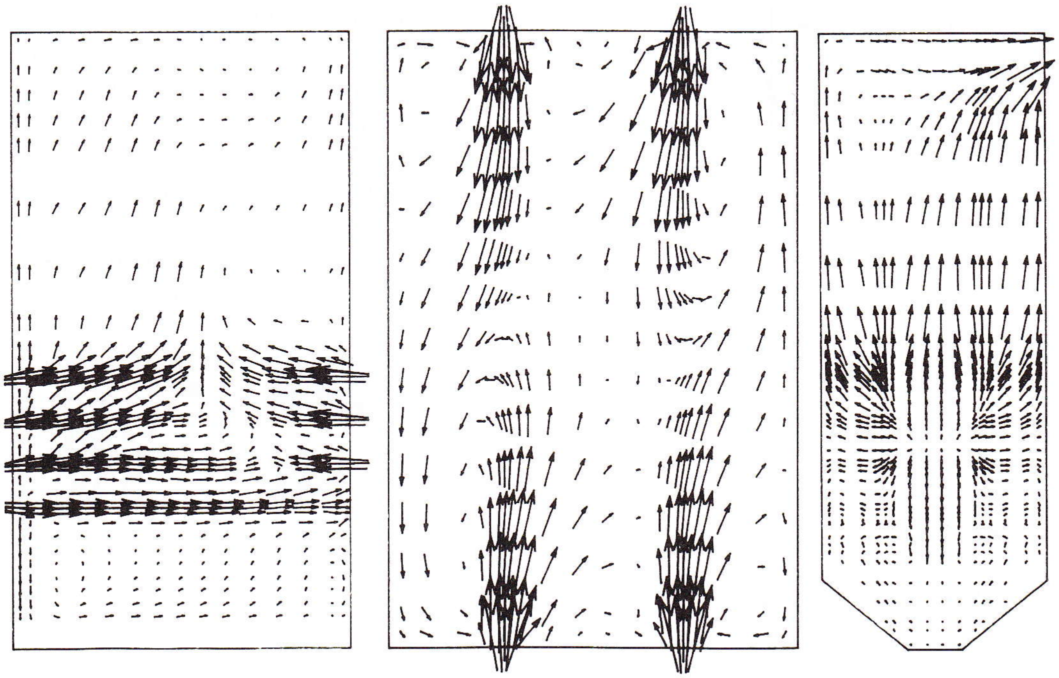

Figure 3 Predicted flow field

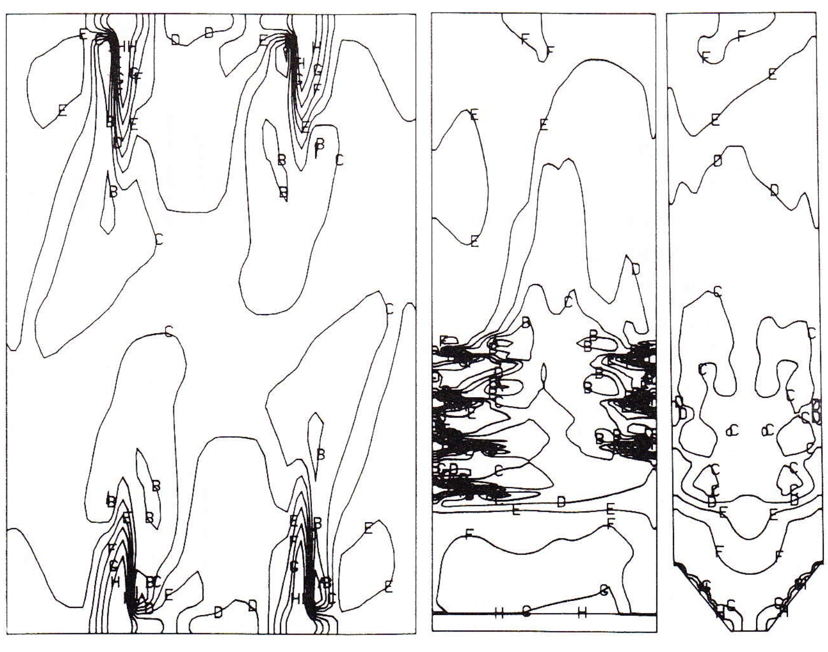

Figure 4 Predicted temperature distribution (K) (A, 2200; B, 2000; C, 1800; D, 1600; E, 1400; F, 1200; G, 1000; H, 800)

where temperatures up to 2000 K are observed. Below the burners the temperatures do not exceed 1400 K and relatively low temperatures prevail in the hopper region. Above the burners temperatures decrease progressively towards the exit to the superheaters due to radiation heat losses to the walls. At the exit to the superheaters mean temperatures are in the range 1200–1400 K which is typical for this kind of boilers.

Gas temperatures were measured by Anson *et al.*[8] who reported having observed temperatures ranging from about 1400 K to 2000 K. However, the location of the measurements is not given preventing quantitative comparisons.

Predicted mixture fraction in the horizontal plane passing through the third level of burners is shown in *Figure 5*. A rich region where mixture fraction exceeds 0.06 extends from each burner to the

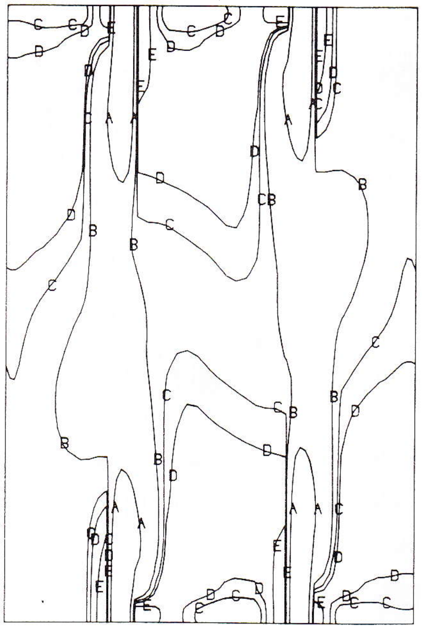

Figure 5 Predicted mixture fraction (A, 0.25; B, 0.08; C, 0.06; D, 0.05; E, 0.03)

opposite one. But since each burner is surrounded by an inlet air port a poor mixture is present close to the front and back walls and in the central region of the furnace.

Oxygen and fuel mass fraction distributions in the same horizontal plane are presented in *Figures 6* and *7* respectively. Higher oxygen concentrations exceeding 0.1 occur near the side walls and are the result of the inlet combustion and atomizing air. In each side wall four regions where the oxygen concentration exceeds 0.1 can be seen, two around each burner. However, since the fuel is introduced through the centre of the burner only two regions of fuel concentration exceeding 0.5 are present in each side wall, one for each burner. As the jets penetrate towards the middle of the furnace oxygen is progressively consumed and concentrations decrease rapidly to values below 0.01.

Soot concentration distribution for the same horizontal plane is shown in *Figure 8*. Soot is produced in rich regions and attains a maximum concentration near the burners, but as the jets penetrate further fuel concentration decreases due to combustion and so does soot production. On the other hand, the presence of oxygen at temperatures above 1400 K leads to oxidation of soot. In the regions where significant fuel concentration exists soot production compensates soot oxidation in such a way that changes in soot concentration are small. In the regions where fuel concentration is small, soot oxidation dominates and so soot concentration decreases.

Predicted radiant heat fluxes at the boiler walls are presented together with the limited experimental data available in *Figure 9*. On the whole, the calculated fluxes agree with the observed ones. The observed differences are in the range of experimental error pointed out by Anson *et al.*[8]. Heat flux meters used in the experimental work have an accuracy of about $\pm 10\%$, but for instruments with a light covering of ash the readings can be in error by up

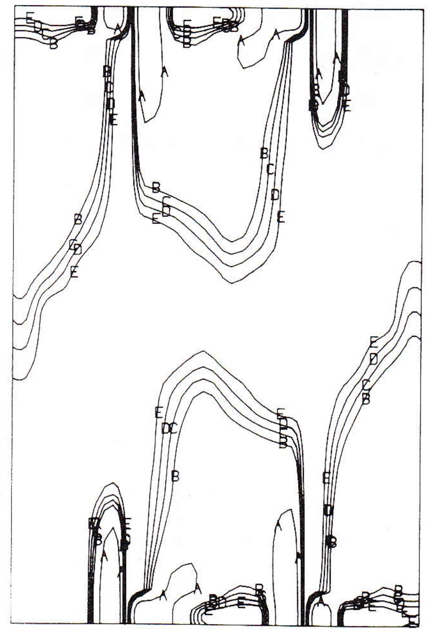

Figure 6 Predicted O_2 mass fraction (A, 0.1; B, 0.04; C, 0.03; D, 0.02; E, 0.01)

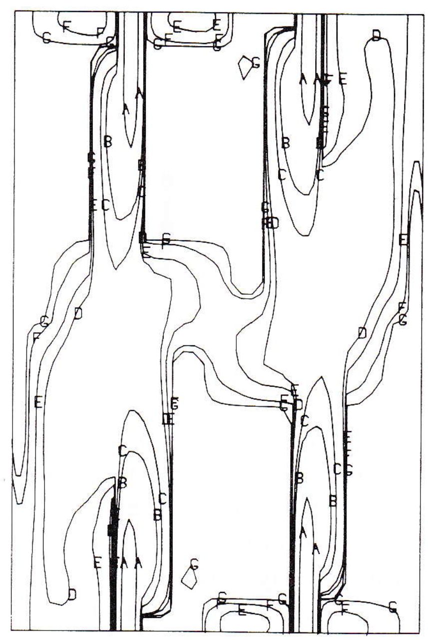

Figure 7 Predicted fuel mass fraction (A, 0.5; B, 0.1; C, 0.05; D, 0.01; E, 0.005; F, 0.001; G, 0.0001)

to 20%. The calculated maximum heat fluxes occur at the front and back walls at the top burner level. The maximum value calculated at the front wall is higher than the experimental one but according to Anson *et al.*[8] the experimental value may be wrong. According to them this may be the result of the downward recirculation of cooler gases induced by the top burner jets, so that the hottest gases occupy a volume in the shape of a vertical short dumb-bell with the neck of the dumb-bell level with the top row of burners. This would allow the heat meters looking toward the neck to see the cooler adjacent gases and walls, whilst the narrow angled optical instruments would still see a centre core of hot luminous gases. The calculated maximum heat fluxes can equal about twice the average value for the enclosure as a whole.

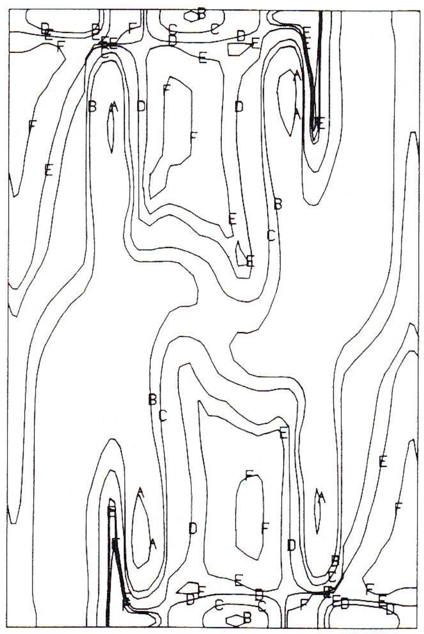

Figure 8 Predicted soot concentration (kg/m³) (A, 5×10^{-3}; B, 10^{-3}; C, 5×10^{-4}; D, 10^{-4}; E, 5×10^{-5}; F, 10^{-5})

CONCLUSIONS

A three-dimensional mathematical model describing the complex phenomena occurring in large boiler furnaces such as turbulent flow, chemical reaction and heat transfer has been presented.

The predictions made for the flow field, temperature, mixture fraction, species concentration and heat flux distribution in an industrial boiler are realistic and supported by the experimental data available. However, more extensive data are required to enable detailed comparisons to be performed.

The results have suggested that 3-D models of the present kind can be used with some confidence for design calculations.

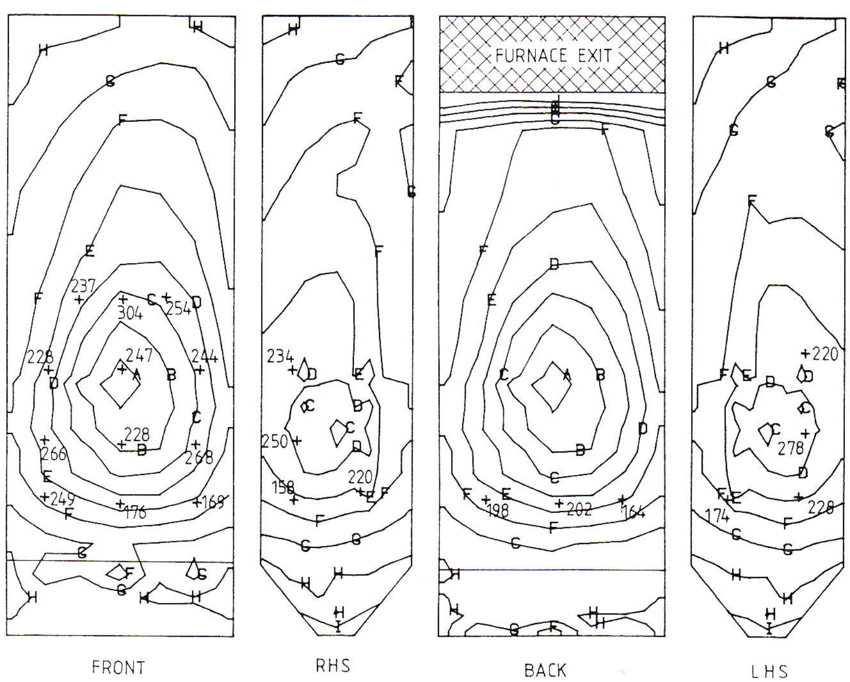

Figure 9 Predicted and measured radiative heat flux at the walls (kW/m²) (A, 350; B, 310; C, 270; D, 230; E, 190; F, 150; G, 110; H, 70; I, 40; J, 10)

REFERENCES

1 Kalmbach, G., Gorner, K. and Seeger, M. Velocity and turbulence measurements by a two-colour-LDA in a furnace model and comparison with a model calculation, *2nd Int. Symp. Applications of Laser Anemometry to Fluid Mechanics, Lisbon* (1984)
2 Shida, H., Adachi, T., Kuragasaki, M., Kunimoto, T. and Hisatome, M. Three-dimensional flow analysis in boiler furnace, *Bull. ASME*, **29**, (247), 136–142 (1986)
3 Shida, H., Karagasaki, M., Adachi, T., Kunimoto, T., Hisatome, M. and Kobayashi, V. Development of three-dimensional numerical analysis method of boiler furnace characteristics. Part 1: Flow analysis, *Technical Review*, Mitsubishi Heavy Industries Ltd., pp. 18–23 (1984)
4 Boyd, R. K., Roscarel, K. J. and Kent, J. H. Gas flow and mixing in a tangentially fired furnace, *3rd Australasian Conf. Heat and Mass Transfer, Melbourne* (1985)
5 Boyd, R. K. and Kent, J. H. Three-dimensional numerical gas flow modelling of boiler furnaces, *8th Australasian Fluid Mechanics Conf.*, pp. 1B14–17 (1983)
6 Benesch, W. and Kremer, H. Mathematical modelling of fluid flow and mixing in tangentially fired furnaces, *20th Symp. (Int.) Combustion*, The Combustion Institute, Pittsburgh, pp. 549–557 (1984)
7 Hirose, T. and Mitunaga, A. An investigation of radiant heat exchange in boiler, *Bull. JSME*, **14**, 829–836 (1971)
8 Anson, D., Godridge, A. M. and Hammond, E. G. Comparison of the calculated and measured heat transfer distribution in an oil-fired water-tube boiler, *J. Inst. Fuel*, pp. 83–90 (June 1974)
9 Lowe, A., Wall, T. F. and Stewart, M. C. A zoned heat transfer model of a large tangentially fired pulverized coal boiler, *15th Symp. (Int.) Combustion*, The Combustion Institute, Pittsburgh, pp. 1261–1270 (1975)
10 Bueters, K. A., Cogoli, J. C. and Habelt, W. W. Performance prediction of tangentially fired utility furnaces by computer model, *15th Symp. (Int.) Combustion*, The Combustion Institute, Pittsburgh, pp. 1245–1260 (1975)
11 Richter, W. and Heap, M. P. The impact of heat release pattern and fuel properties on heat transfer in boilers, *ASME Winter Annual Meeting, Washington, DC* (1981)
12 Xu-Chang, X. Mathematical modelling of three-dimensional heat transfer from the flame in combustion chambers, *18th Symp. (Int.) Combustion*, The Combustion Institute, Pittsburgh, pp. 1919–1925 (1981)
13 Sakai, M., Tokuda, K., Ide, Y., Nakashima, F., Asayama, H. and Aiki, H. Development of three-dimensional numerical analysis method of boiler furnaces characteristics. Part 2: Combustion and heat transfer analysis, *Technical Review*, Mitsubishi Heavy Industries Ltd., pp. 24–34 (1984)
14 Scruton, B., Gibb, J. and Chojnowski, B. Conventional power station boilers: assessment of limiting thermal conditions for furnace-wall tubes, *CEGB Res.*, (17), 3–11 (1985)
15 Robinson, G. F. A three-dimensional analytical model of a large tangentially fired furnace, *J. Inst. Energy*, pp. 116–150 (September 1985)
16 Abbas, A. S., Lockwood, F. C. and Papadopoulus, C. Computation of power station combustors, *ASME 107th Annual Meeting, Anaheim, CA* (1986)
17 Gorner, R. and Zinser, W. Prediction of three-dimensional flows in utility boiler furnaces and comparison with experiments, *ASME 107th Annual Meeting, Anaheim, CA* (1986)
18 Boyd, R. K. and Kent, J. H. Three-dimensional furnace computer modelling, *21st Symp. (Int.) Combustion*, The Combustion Institute, Pittsburgh (1986)
19 Fiveland, W. A. and Wessel, R. A. Numerical model for predicting performance of three-dimensional pulverized-fuel fired furnaces, *ASME Trans. J. Eng. Gas Turbines Power*, pp. 117–126 (1988)
20 De Michele, G., Ghiribelli, L., Pasini, S. and Tozzi, A. A 3-D code for predicting radiative and convective heat transfer in boilers, *26th Nat. Heat Transfer Conf., Philadelphia*, pp. 275–286 (1989)
21 Launder, B. E. and Spalding, D. B. *Mathematical Models of Turbulence*, Academic Press, London (1972)
22 Lockwood, F. C. and Naguib, A. S. The prediction of the fluctuations in the properties of free, round jet, turbulent diffusion flames, *Combust. Flame*, **24**, 109–124 (1975)
23 Lockwood, F. C. and Shah, N. G. A new radiation solution method for incorporation in general combustion prediction procedures, *18th Symp. (Int.) Combustion*, The Combustion Institute, Pittsburgh, pp. 1405–1414 (1981)
24 Khan, I. M. and Greeves, G. A. A method for calculating the formation and combustion of soot in diesel engines, *Heat Transfer in Flames* (Ed. Afgan and Beer), pp. 391–402 (1974)
25 Abbas, A. S., Lockwood, F. C. and Koussa, S. S. The prediction of several residual oil flames, *ASME Paper 81-WA/HT* (1981)
26 Magnussen, B. F. and Hjertager, B. H. On mathematical modelling of turbulent combustion with special emphasis on soot formation and combustion, *16th Symp. (Int.) Combustion*, The Combustion Institute, Pittsburgh, pp. 719–728 (1977)
27 Hottel, H. C. and Sarofim, A. F. *Radiation Transfer*, McGraw-Hill, New York (1967)
28 Truelove, J. S. A mixed grey gas model for flame radiation, *Report HL76/3448/KE*, AERE, Harwell (1976)
29 Spalding, D. B. A novel finite difference formulation for differential expressions involving both first and second derivatives, *Int. J. Num. Meth. Eng.*, **4**, 551 (1972)
30 Caretto, L. S., Gosman, A. D., Patankar, S. V. and Spalding, D. B. Two calculation procedures for steady, three-dimensional flows with recirculation, *Proc. 3rd Int. Conf. Numerical Methods and Fluid Dynamics*, Springer-Verlag, New York, p. 60 (1972)